



Mapping species of submerged aquatic vegetation with multi-seasonal satellite images and considering life history information

Juhua Luo, Hongtao Duan, Ronghua Ma, Xiuliang Jin, Fei Li, Weiping Hu, Kun Shi, Wenjiang Huang

► To cite this version:

Juhua Luo, Hongtao Duan, Ronghua Ma, Xiuliang Jin, Fei Li, et al.. Mapping species of submerged aquatic vegetation with multi-seasonal satellite images and considering life history information. International Journal of Applied Earth Observation and Geoinformation, 2017, 57, pp.154-165. 10.1016/j.jag.2016.11.007 . hal-01594772

HAL Id: hal-01594772

<https://hal.science/hal-01594772v1>

Submitted on 26 Sep 2017

HAL is a multi-disciplinary open access archive for the deposit and dissemination of scientific research documents, whether they are published or not. The documents may come from teaching and research institutions in France or abroad, or from public or private research centers.

L'archive ouverte pluridisciplinaire **HAL**, est destinée au dépôt et à la diffusion de documents scientifiques de niveau recherche, publiés ou non, émanant des établissements d'enseignement et de recherche français ou étrangers, des laboratoires publics ou privés.



Distributed under a Creative Commons Attribution - ShareAlike 4.0 International License

Mapping species of submerged aquatic vegetation with multi-seasonal satellite images considering life history information

JuhuaLuo¹, Hongtao Duan¹, Ronghua Ma^{1,*}, Xiuliang Jin², Fei Li¹, Weiping Hu¹, Kun
Shi¹, Wenjiang Huang³

¹ Key Laboratory of Watershed Geographic Sciences, Nanjing Institute of Geography and
Limnology, Chinese Academy of Sciences, Nanjing 210008, China.

² a UMR EMMAH, INRA, UAPV, 84914, Avignon, France.

³ Key Laboratory of Digital Earth Sciences, Institute of Remote Sensing and Digital Earth,
Chinese Academy of Sciences, Beijing 100094, China.

* Correspondence: rhma@niglas.ac.cn

Abstract: Spatial information of the dominant species of submerged aquatic vegetation (SAV) is essential for restoration projects in eutrophic lakes, especially eutrophic Taihu Lake, China. Mapping the distribution of SAV species is very challenging and difficult using only multispectral satellite remote sensing. In this study, we proposed an approach to map the distribution of seven dominant species of SAV in Taihu Lake. Our approach involved information on the life histories of the seven SAV species and eight distribution maps of SAV from February to October. The life history information of the dominant SAV species was summarized from the literature and field surveys. Eight distribution maps of the SAV were extracted from eight 30 m HJ-CCD images from February to October in 2013 based on the classification tree models, and the overall classification accuracies for the SAV were greater than 80%. Finally, the spatial distribution of the SAV species in Taihu in 2013 was mapped using multilayer erasing approach. Based on validation, the overall classification accuracy for the seven species was 68.4%, and kappa was 0.6306, which suggests that larger differences in life histories between species can produce higher identification accuracies. The classification results show that *Potamogeton malaianus* was the most widely distributed species in Taihu Lake, followed by *Myriophyllum spicatum*, *Potamogeton maackianus*, *Potamogeton crispus*, *Elodea nuttallii*, *Ceratophyllum demersum* and *Vallisneria spiralis*. The information is useful for planning shallow-water habitat restoration projects.

Keywords: Submerged aquatic vegetation (SAV); Mapping; Dominant species; Remote sensing; Life history

40 **1. Introduction**

41 Submerged aquatic vegetation (SAV) has important impacts on the
42 physical, chemical and biological structure and function of aquatic
43 ecosystems, particularly in shallow lakes (Barko et al., 1991; Gumbricht,
44 1993; Hu et al., 2010). Studies indicated that shallow aquatic systems that
45 are dominated by SAV often have better water quality (clarity, total
46 suspended solid, pH, chlorophyll *a* (Chl-*a*), total phosphorus (TP) and total
47 nitrogen (TN) than other systems (Luo et al., 2014), and SAV can cause
48 aquatic ecosystems to shift from a turbid algae-dominated state to a clear-
49 water plant-dominated state (Folke et al., 2004; Soana et al., 2012), because
50 it can inhibit the growth of algae, absorb the excessive nutrients, reduce
51 water currents, accelerate the sedimentation of suspended materials,
52 stabilize sediments and prevent them from re-suspending (Depew et al.,
53 2011; Hilt et al., 2006; Luo et al., 2014; Shuchman et al., 2013). In addition,
54 it can provide food and shelter for wildlife, and habitat for spawning
55 aquatic animals.

56 In recent decades, as a consequence of rapid urbanization and human
57 activities, most of the urban and suburban shallow lakes and rivers in China
58 have experienced accelerating eutrophication followed by the loss or
59 degradation of SAV due to high total suspended matter (TSM)
60 concentration and low water transparency (Duan et al., 2012; Shi et al.,
61 2015). The restoration of SAV in phytoplankton-dominated lakes is crucial
62 for transforming the turbid states of these shallow lakes (Dong et al., 2014;
63 Hilt et al., 2006). In addition, studies have indicated that SAV can help
64 inhibit the growth of phytoplankton by competing for nutrients and light

(Dong et al., 2014; Lombardo and Cooke, 2003). The re-establishment of SAV has been recognized as a valuable ecological engineering technique for improving aquatic systems in China. Efficient SAV restoration planning requires reliable information about the physical habitat requirements of the species (Angradi et al., 2013). For SAV restoration projects, mapping the spatial distribution of the SAV species is important for acquiring the most suitable ecology and environment conditions for the growth of the dominant SAV species. Additionally, an accurate knowledge of the spatial distribution of dominant species of SAV is highly valuable to many scientific and management goals, including the improved parameterization of shallow lake ecosystem processes and models (Zhang et al., 2013).

Surveying the distribution of SAV and species at a large scale is very labour intensive and time-consuming due to the restriction of working in the water environment. Satellite remote sensing techniques have become powerful and effective tools for mapping aquatic vegetation (Liu et al., 2015; Ma et al., 2008; Zhao et al., 2013). For example, Zhao et al. (2013) and Luo et al. (2014) proposed methods for identifying of emergent, floating-leaved and submerged vegetation and mapping their distribution in Taihu Lake using Landsat TM and HJ-1A/1B CCD images, respectively. Robert et al. (2015) developed a satellite-based algorithm to map SAV and then successfully mapped the distribution of SAV in the Laurentian Great Lakes, Lakes Michigan and Ontario. Therefore, multispectral satellite remote sensing can be used to accurately map and identify emergent, floating-leaved and submerged vegetation in shallow coastal waters or lakes due to the large spectral difference among them.

For identifying SAV species, a limited number of exploratory research programs have been conducted using hyperspectral remote sensing data. For example, Han and Rundquist (2003) studied the spectral responses of *Ceratophyllum demersum* at varying depths in both clear and algae-laden

94 water using a hyperspectral hand-held spectroradiometer. Pinnel et al.
95 (2004) gathered airborne hyperspectral remote sensing data for the spectral
96 discrimination of submerged vegetation in Southern Germany. Yuan and
97 Zhang (2006) investigated the spectral characteristics of the SAV plant
98 species *Potamogeton crispus*, *Myriophyllum spicatum* and *Potamogeton*
99 *malaianus* with the same coverage and found that their red edge peaks and
100 valleys are different. These studies suggested that there are tiny spectral
101 differences among SAV species, and it is only possible to recognize them
102 using hyperspectral remote sensing data with abundant spectral
103 information.

104 However, considering the cost and availability of hyperspectral
105 satellite data, it is infeasible to use them to continuously monitor and
106 identify SAV species. It appears to be impossible to map and identify SAV
107 species using only multispectral satellite image because the spectral
108 differences among the SAV species are tiny and therefore difficult to
109 capture using broadband remote sensing data. Fortunately, different SAV
110 species have different phenological characteristics and life histories, which
111 has made it possible to map and identify SAV species using multiseasonal
112 and multispectral satellite remote sensing data based on information on
113 their life histories, and it has been proven to be effective to identify
114 terrestrial vegetation types based on multi-temporal satellite remote
115 sensing data (Leite et al., 2011; Liu et al., 2006; Murthy et al., 2003) and
116 phenological information. However, the method has not been used and
117 tested for mapping aquatic vegetation species.

118 Therefore, in this study, using ArcGIS spatial analysis technology, we
119 developed a multilayer erasing flow for mapping SAV species in Taihu
120 Lake by combining their life history characteristics and multi-seasonal
121 satellite remote sensing data. To our knowledge, it is the first study to map
122 the dominant SAV species using satellite images.

2. Materials and methods

2.1. Study area

Taihu Lake (30°55'40"– 31°32'58"N, 119°52'32"– 120°36'10"E) is one of the five largest freshwater lakes in China and covers an area of approximately 2,338 km². It is located at the core of the Yangtze Delta in the lower reaches of the Yangtze River in eastern China (Figure 1). Taihu Lake is a typical shallow lake with a maximum depth of less than 3 m and an average depth of 1.9 m. The western and central parts of Taihu Lake belong to the algal-dominated zone, where the waters are consistently extremely turbid with high total nitrogen (TN), total phosphorus (TP) contents and suspended matter concentration. Algal blooms occur frequently in the algal-dominated zone (Duan et al., 2015). The eastern of Taihu Lake, including Meiliang, Gonghu, Zhenhu, Guhuanghu, Xukou, Doangshan and Dongtaihu Bays, are covered with hydrophytes and therefore belonged to a macrophyte-dominated zone with much lower TN and TP content and higher water transparency than did those in the algal-dominated zone (Luo et al., 2016). According to previous studies (Carr et al., 2010; Liu et al., 2015), no aquatic vegetation exists at water depth greater than 2.3 m in the Taihu Lake. Therefore, we exacted the region with water depths less than 2.3 m as the study area. Depth data was provided by Taihu Laboratory for Lake Ecosystem Research (Figure 1).

There are four types of aquatic vegetation in the grass-type zone: emergent, free-floating, floating-leaving and submerged vegetation. Emergent and free-floating hydrophytes accounts for less than 5% of the total aquatic vegetation area and are mostly distributed in the littoral zone of Taihu Lake (Luo et al., 2014). In this study, we divided aquatic vegetation into floating-leaved and submerged vegetation. According to field survey and documentary records, there are approximately 17 SAV

species in Taihu Lake, but only seven species are dominant: *Elodea nuttallii*, *Potamogeton crispus*, *Myriophyllum spicatum*, *Potamogeton maackianus*, *Ceratophyllum demersum* and *Vallisneria spiralis* (Ma et al., 2008; Qin, 2008; Ye et al., 2009).

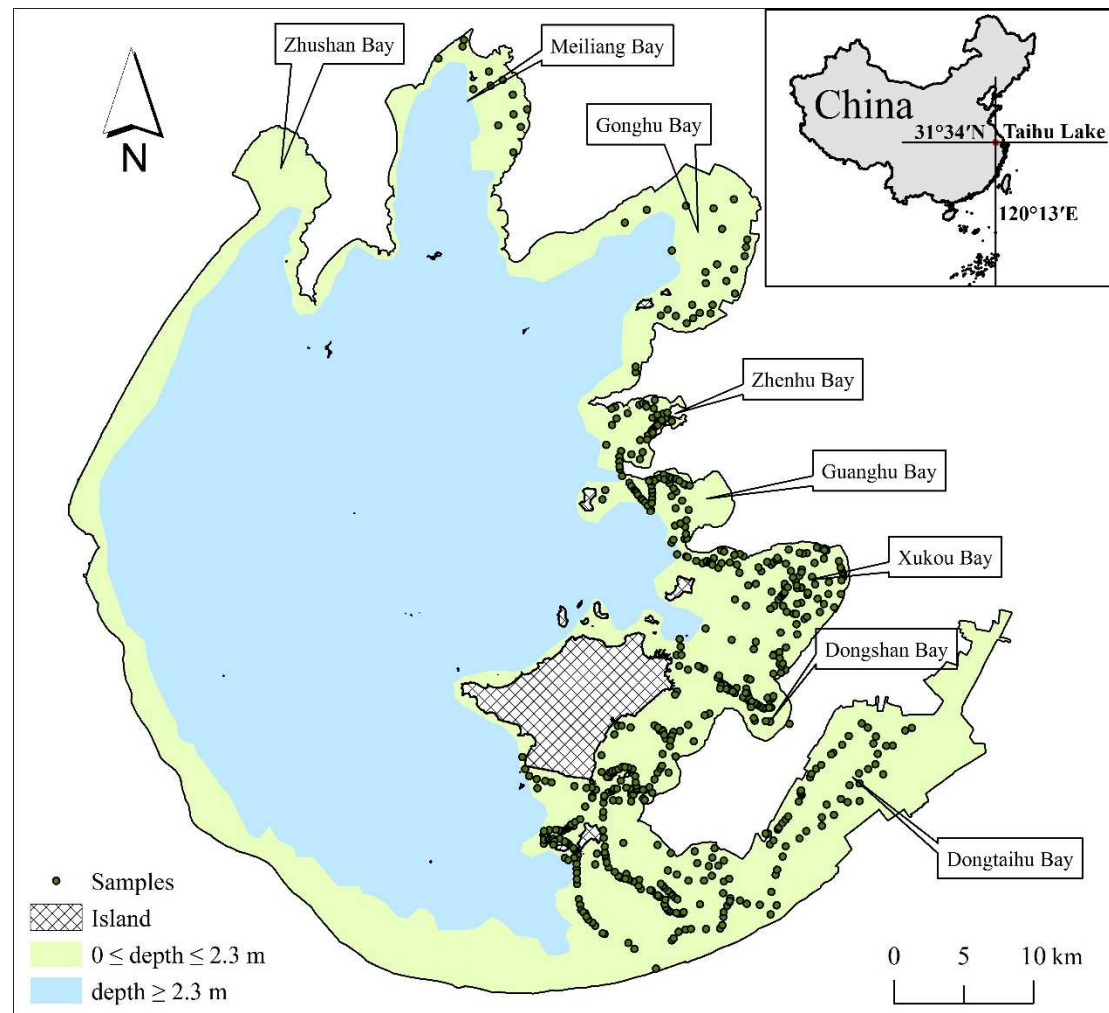


Figure 1. Location of Taihu Lake within China (depth data was provided by Taihu Laboratory for Lake Ecosystem Research)

2.2. Field data collection

Field surveys were conducted on 10–14 March, 22–24 May, 10–13 July, 17–22 August and 23–26 September in 2013. A total of 604 ground-truth samples were collected for open water and aquatic vegetation (100 samples in March, 102 samples in May, 112 samples in July, 143 samples in August and 179 samples in September) in macrophyte-dominated zone of Taihu

Lake (Figure 1), including 405 submerged vegetation samples and 231 floating-leaved vegetation samples. The aquatic vegetation sampling plots were limited to areas measuring at least 60×60 m (*i.e.*, four pixels of an HJ-CCD image) and that had a relatively uniform distribution of vegetation. We used a portable GPS receiver with an accuracy of 3 m to record the centre coordinates of each sample and recorded the type and percent coverage of aquatic vegetation. We also used GPS to record the boundary extent of the representative floating-leaved and submerged aquatic vegetation sample regions to generate a polygon vector file.

2.3. Remote sensing data collections and processing

HJ-CCD images recorded from the HJ-1A/1B CCD cameras were acquired from the China Centre for Resources Satellite Data and Application (CRESDA). These cameras were onboard the HJ-1A and HJ-1B satellites, which were launched by CRESDA on September 6, 2008. Their spectral ranges and spatial resolutions are similar to those of the first four bands of Landsat TM. The single CCD imagery width is 360 km, and the two satellites constellation provides a wider swath width (700 km) and a re-visit time of 48 h (two days). Its high re-visit cycle was of great importance for mapping the dominant SAV species in this study.

In this study, eight cloud-free and sun glint free HJ-CCD images covering Taihu Lake and acquired on February 20, March 12, April 25, May 22, July 11, August 16, September 26 and October 28, 2013 were used, respectively. The ENVI software package was used to pre-process the remote sensing images. Radiometric corrections were made using coefficients from the metadata accompanying the images (*e.g.*, gains and offsets). FLAASH uses a robust procedure to correct for atmospheric attenuation and adjacency effects (Module, 2009). Four key input parameters for the FLAASH module included: the mid-latitude atmosphere model, urban

aerosol model, atmosphere water vapour and visibility. Based on the location of the study area covered by the scenes and the satellite transit time, the first two parameters were easily determined. However, water vapour and visibility values may vary between the images, and these were determined by trial-and-error until a typical spectral pattern of plants was observed (Pu et al., 2012). The HJ-CCD images were also geometrically corrected with a previously corrected Landsat TM image with a geometric accuracy of < 0.5 pixels.

2.4. Life histories of dominant species of SAV in Taihu Lake

There are seven dominant SAV species in Taihu Lake: *Potamogeton crispus*, *Elodea nuttallii*, *Myriophyllum spicatum*, *Potamogeton maackianus*, *Ceratophyllum demersum*, *Vallisneria spiralis* and *Potamogeton malaianus*. Using references and field surveys, the life histories of the seven dominant species are summarized in Figure 1. Detailed descriptions of the species are now discussed. 1) *Potamogeton crispus* can tolerate temperatures below 0°C and can survive over winter. It grows rapidly after March, reaches a maximum biomass in mid-May and then soon dies and becomes dormancy (Nichols and Shaw, 1986; Rogers and Breen, 1980). It regrows after November. 2) *Elodea nuttallii* tolerates temperature below 0°C and can survive over winter, forming a dense mat of vegetation just above the lake bottom (Oki, 1994). It grows rapidly after May, reaches a maximum biomass in early July, and then soon died and becomes dormancy. It regrows after September (Kunii, 1984). 3) *Potamogeton maackianus* cannot survive over winter. It begins to rapidly grow in early April and reaches a maximum biomass in July, grows slowly and gradually withers (Ni, 2001). 4) *Myriophyllum spicatum* cannot survive over winter. It grows rapidly from April to July and reaches its peak stage from early July to early August. It begins its dormancy from December to the following February (Nichols and Shaw, 1986). 5)

Ceratophyllum demersum cannot survive over winter and starts dormancy between December to following February. It grows rapidly from early June and reaches a maximum biomass from late August to early September, and then grows slowly and gradually withers (Best, 1977). 6) *Vallisneria spiralis* cannot survive over winter and is dormant from December to next February. It begins growing slowly from April and grows rapidly during July-September, after which it reaches maximum biomass during early October to mid-October. 7) *Potamogeton malaianus* has a similar life history, except for its peak stage. It reaches maximum biomass from late October to early November (Liu et al., 2007; Wiegleb and Kadono, 1989; Xiao et al., 2010).

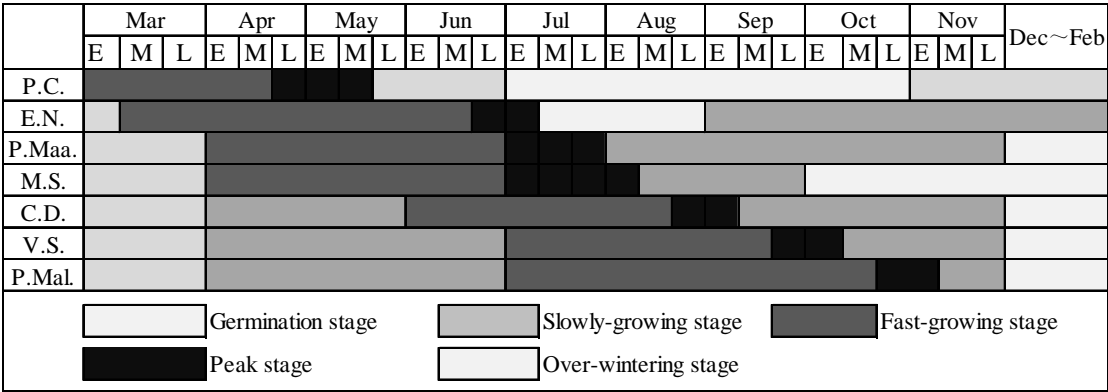


Figure 2. Life histories of seven SAV species in Taihu Lake

Note: *P.C.*=*Potamogeton crispus*; *E.N.*=*Elodea nuttallii*; *M.S.*=*Myriophyllum spicatum*; *P.Maa.*=*Potamogeton maackianus*; *C.D.*=*Ceratophyllum demersum*; *V.S.*=*Vallisneria spiralis*; *P. Mal.*=*Potamogeton malaianus*; E=Early; M=Middle; L=Late.

2.5 Methods

2.5.1. Classification tree model for the extraction of SAV

Classification tree (CT) analyses are based on the dichotomous partitioning of data at certain thresholds of the value of the explanatory variables, which determine the branch a particular sample will follow (Olshen and Stone, 1984). It is considered to be especially robust when

used with a small sample size of remotely-sensed data (Tadjudin and Landgrebe, 1996). Luo et al., (2014) developed a classification tree for mapping floating-leaved and submerged vegetation in Taihu Lake. As shown in Fig. 3, in the classification tree, floating-leaved vegetation was first extracted from other types using the floating-leaved vegetation sensitive index (FVSI), and then the submerged vegetation sensitive index (SVSI) was used to distinguish between the SAV and water. The FVSI and SVSI were defined as:

$$FVSI = PC_2 \quad \text{Eq. (1)}$$

where PC_2 is the second principal component of the principal component transform.

$$SVSI = TC_1 - TC_2 \quad \text{Eq. (2)}$$

where TC_1 and TC_2 are, respectively, the first and second components of the tasseled cap transform, which are also called the brightness and greenness (Crist, 1985; Healey et al., 2005).

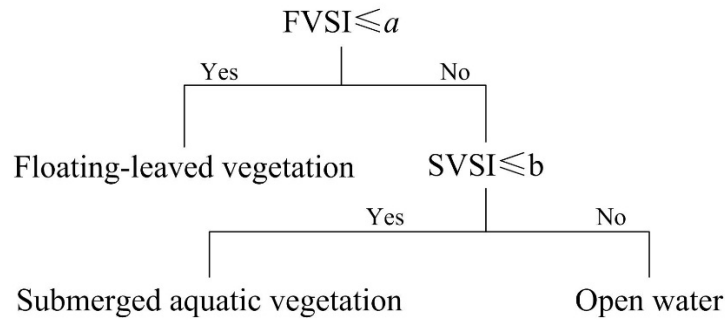


Figure 3. Classification tree of identifying floating-leaved vegetation and submerged aquatic vegetation based on FVSI and SVSI, where a and b are the threshold of FVSI and SVSI

In the classification tree, the thresholds, i.e., a and b , of FVSI and SVSI vary with images, because they can be influenced by aquatic vegetation conditions, environmental and physical conditions. For the image with the synchronously collected ground samples, the thresholds of FVSI and SVSI were determined and modified slightly based on field

survey points until the maximum classification precision was achieved. For the image without the synchronously collected ground samples, Luo et al. (2014) developed an effective algorithm to calculate the thresholds. In this study, the thresholds of FVSI and SVSI in the CT models for the image acquired on July 11 were obtained using the synchronously collected ground samples, whereas the thresholds for the images without synchronously collected ground samples were calculated according to the thresholds for the July 11 image using the algorithm developed by Luo et al. (2014) The algorithms can be expressed as:

$$CT_m_FVSI = k \times CT_FVSI + h \quad \text{Eq. (3)}$$

$$CT_m_SVSI = p \times CT_SVSI + q \quad \text{Eq. (4)}$$

where CT_m_FVSI and CT_m_SVSI are the thresholds of FVSI and SVSI in the classification model, respectively, for the image acquired at time m in the absence of ground samples, which should be calculated, that is a and b in the classification tree in Figure 3; and CT_FVSI and CT_SVSI are the thresholds of FVSI and SVSI in the classification model, respectively, for the image of July 11. The CT_FVSI and CT_SVSI were obtained using the field survey data. For k and h , we first selected the same regions of interest (ROIs) with floating-leaved vegetation from the images at time m and July 11, respectively. Secondly, two group FVSI values derived from the two ROIs were placed in descending order. Finally, the line fitting model was simulated using the two descending FVSI datasets, and the slope and intercept of the linear model were k and h , respectively. In a similar way, the line fitting model could be simulated by the two groups of SVSI in descending order, and then we can acquire p and q . See the work by Luo et al. (Luo et al., 2014) for the detailed test and validation of the algorithm. The thresholds and classification accuracies of SAV were assessed by the overall classification accuracy (OCA) (Luo et al., 2016; Luo et al., 2014).

2.5.2. Method for identifying dominant species of SAV

Based on the life history information of the dominant SAV species, the dominant species were identified from the time-series SAV distribution maps using the erase tool in the analysis tool of ArcGIS. The erase tool is an important analysis tool in ArcGIS. As shown in Figure 4, erase creates a new feature class by overlaying two sets of features. The erase features polygons that define the erasing area. The input features or portions of input features that overlap the erase features are not written to the output feature class. The input features can be points, lines or polygons, but the erase features must be polygons. The output features will be of the same geometry type as the input Features. Input features or portions of input features that do not overlap erase features are written to the output feature class.

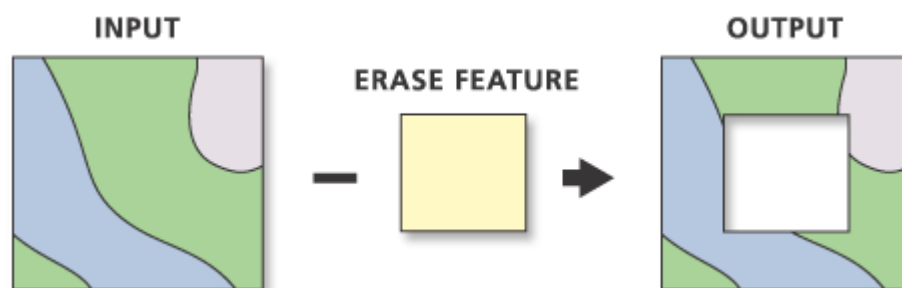


Figure 4. Schematic diagram of erase tool (from ArcGIS desktop help)

Figure 5 shows the flow chart and methods that were used to identify the dominant SAV species. As shown in Figure 5, Layers 2, 3, 5, 7, 8, 9 and 10 are the SAV spatial distribution maps derived from the images of February 20, March 12, May 22, July 11, August 16, September 26 and October 28 based on the classification tree models. The methods were developed according to the following general principles. 1) The dominant species were extracted successively according to the time order of the maximum biomass from January to December, and thus, *Potamogeton crispus*, *Elodea nuttallii*, *Myriophyllum spicatum*, *Potamogeton*

319 *maackianus*, *Ceratophyllum demersum*, *Vallisneria spiralis* and
320 *Potamogeton malaianus* were extracted in sequence. 2) the Erase tool in
321 ArcGIS was used to extract the species. The input layer and erase feature
322 are SAV layers extracted from the images using the corresponding
323 classification tree models. To obtain the distribution layer of a species layer,
324 the input layer was derived from the image during the fast-growing and
325 peak stages of the species, and the erase feature was derived from the image
326 between the germination and slow growth stages of the species. Because
327 the species has the highest coverage and was the closest to water surface in
328 their fast-growing and peak stages, during which they can be readily
329 captured by remote sensing. In the germination and slow growth stages,
330 the species' canopies are not close to the water surface and coverage are
331 low; in these stages, very little species information can be captured by
332 remote sensing, especially in high suspended shallow lakes.

333 Therefore, based on the life histories of the seven SAV species, the
334 detailed steps for extracting the seven species are as follows: 1) extraction
335 of *Potamogeton crispus*. From February to March, *Potamogeton crispus*
336 and *Elodea nuttallii* are in the fast-growing stage, and in the germination
337 stage in July, they are the main dominant species in Taihu. The SAV layers
338 derived from March and April were merged, and then the merged layer was
339 used as the input layer, the SAV layers from July were used as the erase
340 feature, and therefore the output layer was the distribution layer of
341 *potamogeton crispus*; (2) extraction of *Elodea nuttallii*. The SAV layers
342 derived from February and March were merged, the merged layer was used
343 as the input layer, *Potamogeton crispus* layer was used as the erase feature,
344 and therefore the output layer was the distribution layer of *Elodea nuttallii*;
345 (3) extraction of *Potamogeton maackianus*. *Potamogeton maackianus* is in
346 the fast-growing stage in May and in the slowly-growing stage in March.
347 Therefore the SAV layer in May was used as the input layer; the SAV layer

in March and *Potamogeton crispus* and *Elodea nuttallii* layers were merged, the merged layer was used as the erase feature, and the output layer was the distribution layer of *Potamogeton maackianus*; (4) extraction of *Myriophyllum spicatum*. This species is in its peak stage in July and in the slowly-growing stage in October. The SAV layer in July was used as the input layer; the SAV layer in October and the layers of *Potamogeton crispus* and *Elodea nuttallii* and *Potamogeton maackianus* were merged, the merged layer was used as the erase feature, and the output layer was the distribution layer of *Myriophyllum spicatum*; (5) extraction of *Ceratophyllum demersum*. This species is in its fast-growing stage in August and in the slowly-growing stage in late-October. The SAV layer in August was used as the input layer, the SAV layer in late-October and the layers of *Potamogeton crispus*, *Elodea nuttallii*, *Potamogeton maackianus* and *Myriophyllum spicatum* were merged, the merged layer was used as the erase feature; and the output layer was the distribution layer of *Ceratophyllum demersum*; (6) extraction of *Vallisneria spiralis*. This species is in its fast-growing stage in September and in the slowly-growing stage in late-October. The SAV layer in August was used as the input layer, the SAV layer in late-October and the layers of *Potamogeton crispus*, *Elodea nuttallii*, *Potamogeton maackianus*, *Myriophyllum spicatum* and *Ceratophyllum demersum* were merged, the merged layer was used as the erase feature, and the output layer was the distribution layer of *Vallisneria spiralis*; (7) extraction of *Potamogeton malaianus*. All of the SAV layers from February, March, April, May, July, August, September and October were merged, the merged layer was used as the input layer, the classification layers of the other six species were merged, the merged layer was used as the erase feature, and the output layer was the distribution layer of *Potamogeton malaianus*.

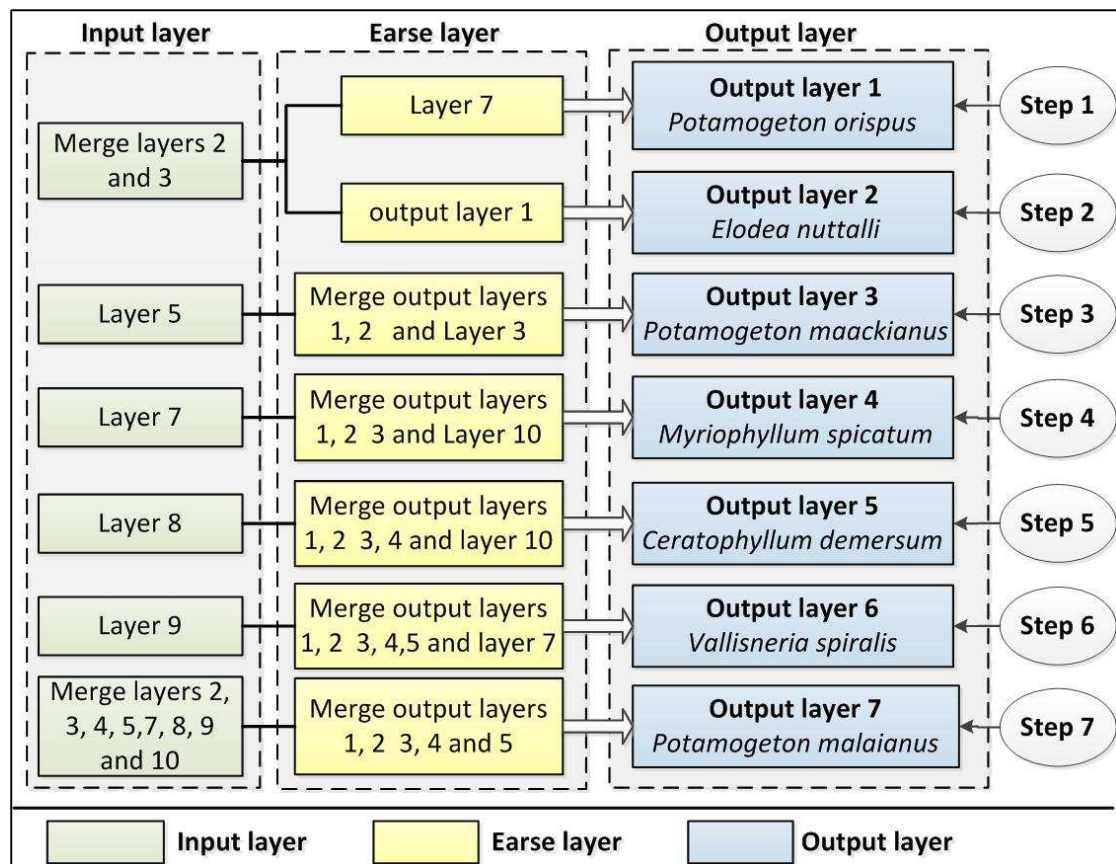


Figure 5. Flow chart for identifying seven SAV species

Note: Layer 2, 3, 4, 5, 7, 8, 9, 10 are the SAV distribution maps were derived from the image of February 20, March 12, April 25, May 22, July 11, August 16, September 26 and October 28, 2013 using classification tree models.

According to Figure 5, the spatial distribution of the seven SAV species in 2013 can be mapped in shallow lakes. Classification accuracies of dominant SAV species were assessed by producer's accuracy (PA), user's accuracy (UA), overall accuracy (OA) and Kappa (Congalton et al., 1983). Meanwhile, to analyse the dominant species in different seasons, we merged the SAV layers from 20 February, 12 March and 25 April 2013 as the SAV distribution layer in the spring. By combining the spatial distribution map of the seven species in 2013 and the SAV distribution layer in the spring, the spatial distribution map of the dominant species in the spring can be obtained. The SAV layers from 22 May and 11 July 2013 were merged as the SAV distribution layer in the summer, and the SAV layers from 16 August, 26 September and 28 October 2013 were merged

as the SAV distribution layer in the autumn. In the same way, the spatial distribution maps of the dominant species in the summer and autumn were built.

3. Results

3.1. Identification of aquatic vegetation

Using Eqs. (1) and (2), FVSI and SVSI were derived from the image of July 11, 2013. Then, the FVSI and SVSI values of the samples collected from 11-13 July 2013 were obtained. Based on the FVSI and SVSI values of the different types, the histogram was obtained, and then the optimal thresholds of FVSI and SVSI were quantitatively determined. As shown in Figure 6, the floating-leaved vegetation could be identified from the other two types when $FVSI \leq -0.035$, and then the threshold ($SVSI=0.192$) could be used to distinguish the submerged aquatic vegetation from the water. Using the optimal thresholds and classification tree, the floating-leaved vegetation and submerged aquatic vegetation on 11 July 2013 were mapped (Figure 7).

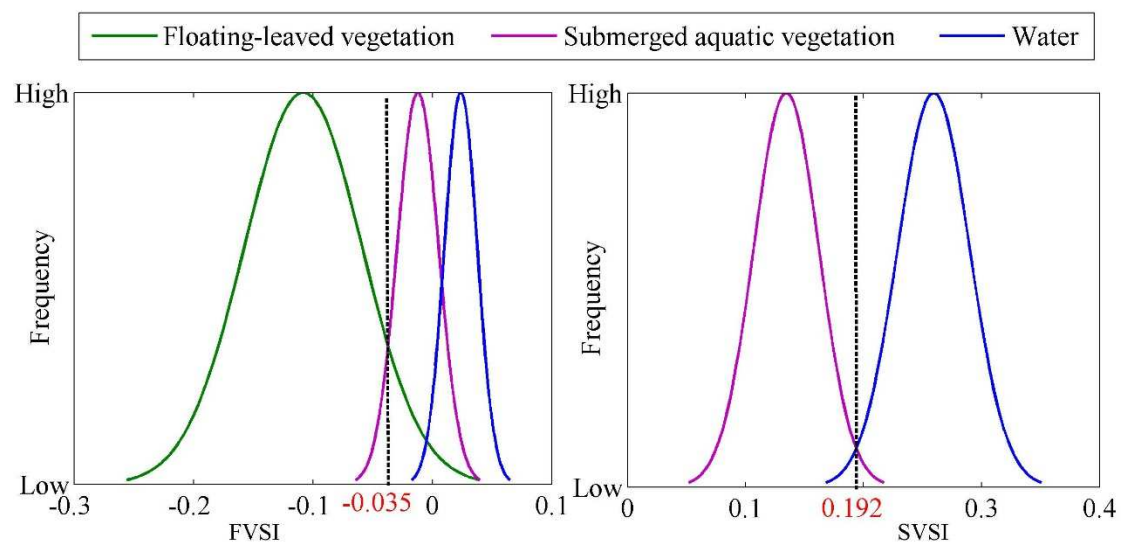


Figure 6. Histogram of FVSI and SVSI from different types

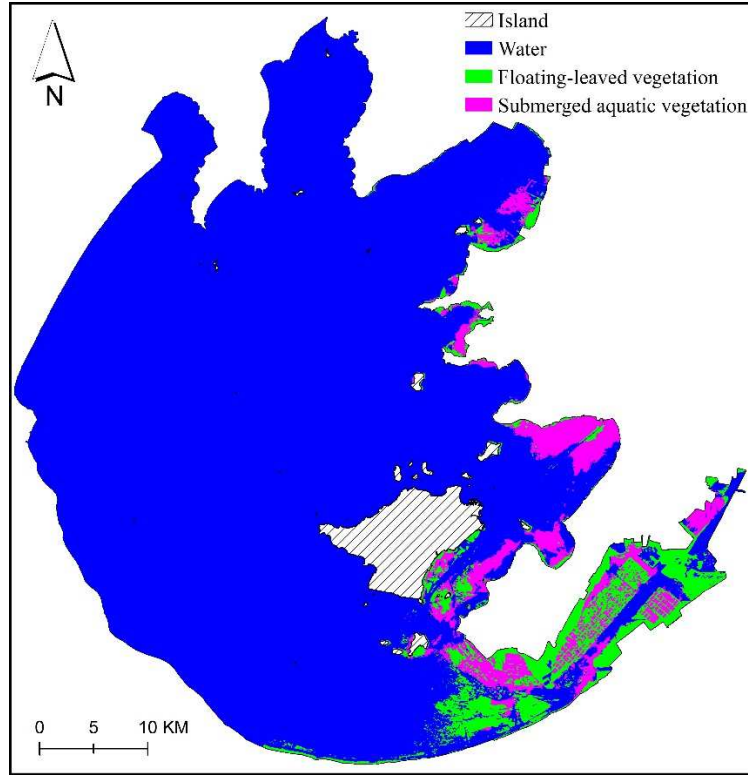


Figure 7. Spatial distribution map of aquatic vegetation on July 11, 2013

Next, based on the threshold of FVSI and SVSI for July 11, 2013, we calculated all of the thresholds of FVSI and SVSI for the other images using the algorithms (Eqs. (3) and (4)) (Table 1). The classification results for March 12, May 13, July 13, August 16, September 26 and October 28 were validated using the corresponding ground samples. The results show that the overall classification accuracies were higher than 80%, and that 83% of the misclassified samples had a coverage < 20 %, and therefore might be difficult to identify SAV with a coverage < 20% using satellite images with resolutions of 30 m.

Table 1. Thresholds of FVSI and SVSI in classification trees. a and b are the thresholds of FVSI and SVSI, respectively. OA = Overall accuracy.

Date	a	b	OA (%)	Date	a	b	OA (%)
20-Feb-13	-0.055	0.337	—	11-Jul-13	-0.035	0.192	82.1
12-Mar-13	-0.055	0.318	88.7	16-Aug-13	-0.075	0.129	85.7
25-Apr-13	-0.025	0.194	—	26-Sep-13	-0.063	0.174	84.4
22-May-13	-0.035	-0.200	85.9	28-Oct-13	-0.038	0.160	—

Eight classification trees for the eight images were established, and therefore eight SAV distribution layers were obtained (Figure 8). As shown

in Figure 8, the SAV was distributed mainly in the eastern bays of Taihu Lake. In February and March, there was a small amount of SAV in Meiliang and Dongtaihu Bays. From April to May, SAV existed mainly in Xukou, Dongshan and Dongtaihu Bays. The SAV distribution area gradually increased in Xukou and Dongtaihu Bays from July to October.

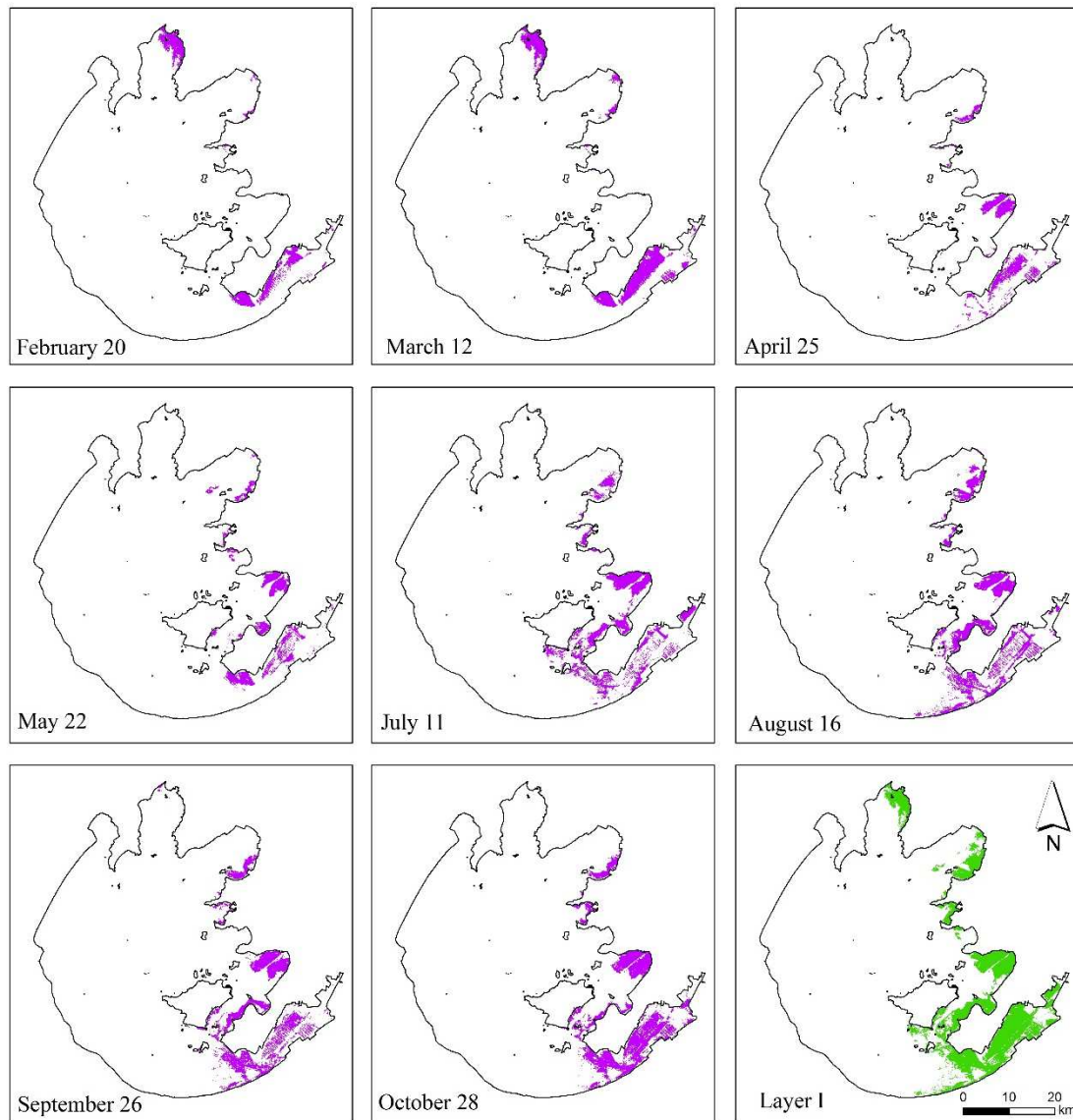


Figure 8. Spatial distribution maps of SAV with different times in 2013 in Taihu Lake
Note: Layer I is the distribution map of SAV in 2013 by merging the SAV layers of February 20, March 12, April 25, May 22, July 11, August 16, September 26, October 28.

Figure 9 shows that the area covered by SAV increased from 60.27 km² in February to 163.49 km² in September. From February 20 to October

28, the region covered by SAV in every bay changed with time because of the different life histories of the different SAV species (Figure 9). Altogether, the total area covered by SAV was 291.02 km² in 2013.

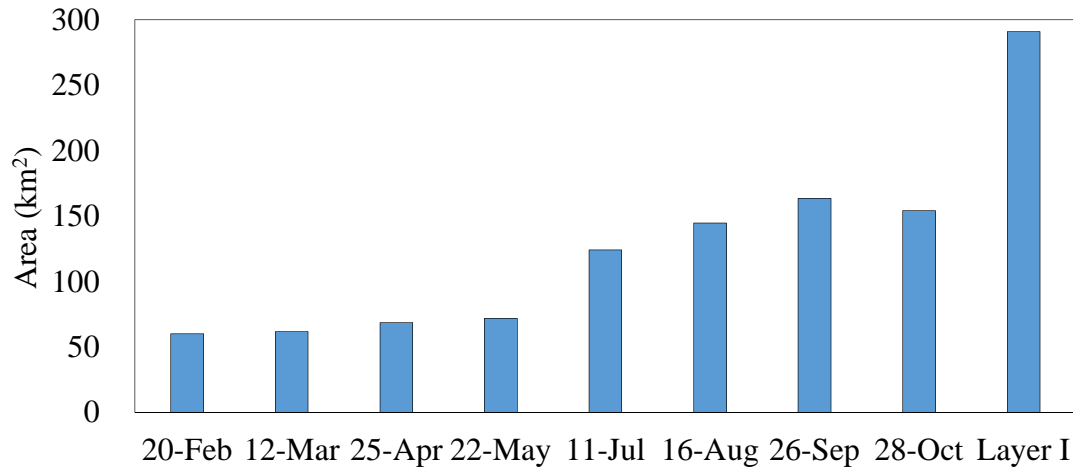


Figure 9. Distribution areas of SAV from different times in 2013

3.2. Mapping dominant species of SAV

Based on the eight distribution maps of SAV in 2013 and the method for identifying the dominant species of SAV shown in Figure 8, the classification map with seven dominant SAV species in 2013 was obtained and is shown in Figure 10.

The accuracy of the classification map was assessed using an error matrix (Table 2). The overall accuracy was 68.4%, and kappa was 0.6306. *Potamogeton crispus* and *Elodea nuttallii* have distinct life histories with other species, and they therefore had high classification accuracies with PA of 75.5% and 70.2%, and UA of 78.4% and 74.1%, respectively. However, there were large misclassifications between *Potamogeton crispus* and *Elodea nuttallii* due to their similar life histories. *Potamogeton malaianus* and *Potamogeton maackianus* exhibited classification accuracies greater than 68%, followed by *Myriophyllum spicatum* and *Vallisneria spirali*. *Ceratophyllum demersum* had the lowest classification accuracy with PA of 62.7% and UA of 60.4%, respectively, due to its small proportion in

Taihu Lake and inconspicuous life history. Due to their similar life histories, there were large misclassification between *Potamogeton malaianus* and *Vallisneria spirali*, between *Myriophyllum spicatum* and *Potamogeton maackianus*.

Table 2. Accuracy assessment of classification results for seven SAV species, PA = % Producer's accuracy; UA = % User's accuracy.

	Species	Predicted							Total	PA
		P.C.	E.N.	P.Maa.	M.S.	C.D.	V.S.	P.Mal.		
Measured	P.C.	40	5	2	1	2	1	2	53	75.5
	E.N.	6	40	2	3	3	2	1	57	70.2
	P.Maa.	2	1	42	6	4	2	4	61	68.9
	M.S.	0	2	6	43	5	4	4	64	67.2
	C.D.	0	3	3	6	32	4	3	51	62.7
	V.S.	2	1	2	3	4	34	6	52	65.4
	P.Mal.	1	2	4	4	3	7	46	67	68.7
	Total	51	54	61	66	53	54	66	405	
	UA	78.4	74.1	68.9	65.2	60.4	63.0	69.7		
Overall accuracy= 68.4%; Kappa= 0.6306										

Note: P.C. = *Potamogeton crispus*; E.N. = *Elodea nuttallii*; M.S.= *Myriophyllum spicatum*; P.Maa. = *Potamogeton maackianus*; C.D.= *Ceratophyllum demersum*; V.S.= *Vallisneria spiralis*; P. Mal.= *Potamogeton malaianus*.

As shown in Figures 10 and 11, *Potamogeton malaianus* was the most widely distributed species in Taihu Lake and constituted 28.3% of the total SAV. *Myriophyllum spicatum* was the second most widely distributed species, with a percentage of 16.6% of the total SAV, and was distributed in Gonghu, Xukou, Dongtaihu Bays and the east coast of Xishan island. *Potamogeton maackianus* accounted for 15.1% of the total SAV and was mainly distributed in Xukou and Dongshan Bays. *Potamogeton crispus* was mainly distributed in Meiliang Bay in the form of single dominant species and Dongtaihu Bay in the form of accompanying species, and it constituted 15.8% of the total SAV. *Elodea nuttallii* was mainly distributed in Dongtaihu Bay, and constituted 8.9% of the total SAV. *Ceratophyllum demersum* and *vallisneria spiralis* accounted for 8.0% and 7.1% of the total SAV, respectively. *Ceratophyllum demersum* was scattered in the bays

with the exception of Meiliang and Guanghu Bays and *Vallisneria spiralis* was mainly distributed in Dontaihu Bay.

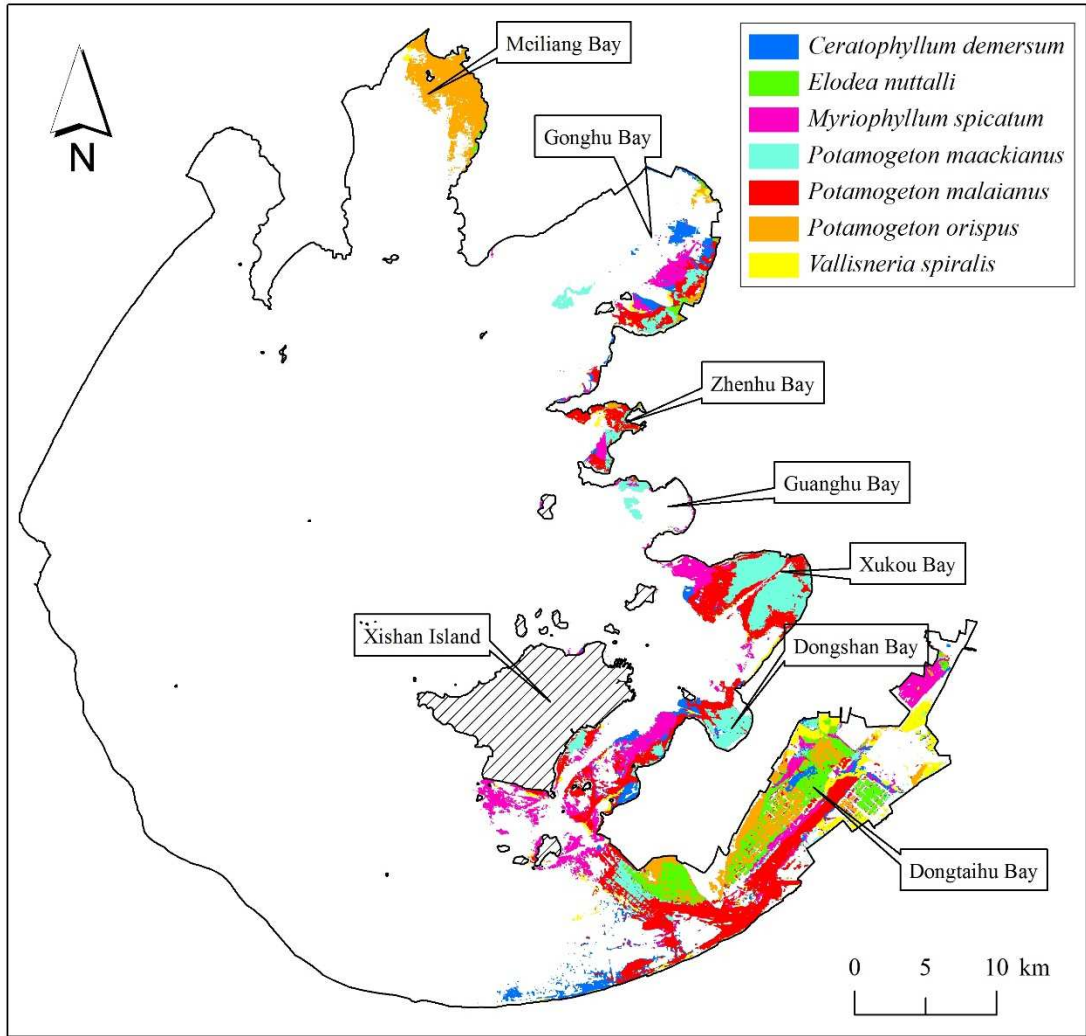


Figure 10. Distribution map of seven SAV species in 2013 in Taihu Lake

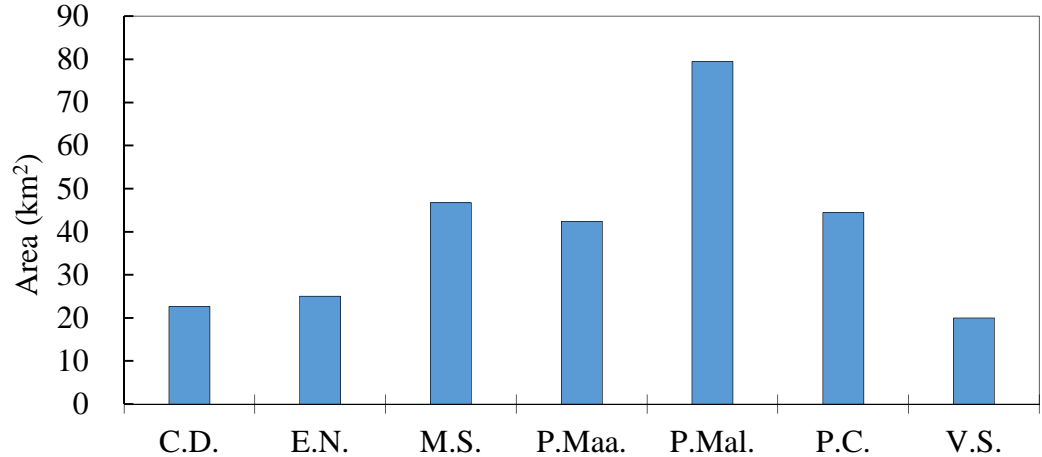


Figure 11. Distribution area of seven SAV species in 2013 in Taihu Lake

Note: P.C.=*Potamogeton crispus*; E.N.= *elodea nuttallii*; M.S. = *Myriophyllum spicatum*;
P.Maa.=*Potamogeton maackianus*; C.D.=*Ceratophyllum demersum*; V.S.=*Vallisneria spiralis*;
P. Mal.=*Potamogeton malaianus*.

Figure 12 shows the spatial distribution of the dominant SAV species in spring, summer and autumn. The distribution area of seven species changed with the seasons. In the spring, the dominant SAV species were *Potamogeton crispus*, *Elodea nuttallii* and *Potamogeton maackianus*, and they were mainly distributed in Meiliang, Xukou and Dongtaihu Bays. In the summer, *Myriophyllum spicatum*, *Potamogeton maackianus* and *Potamogeton malaianus* were primary dominant species. In the autumn, *Potamogeton malaianus* was covered the largest area and was the most widely distributed species, followed by *Potamogeton maackianus*, *Elodea nuttallii*, *Myriophyllum spicatum*, the remaining species. The distribution rule of the species with seasons is consistent with their life histories, which was further evidence that the method proposed was reliable. As shown in Figure 13, the area covered by SAV was largest in the autumn (212.9 km²), followed by summer (153.5 km²) and spring (122.1km²)

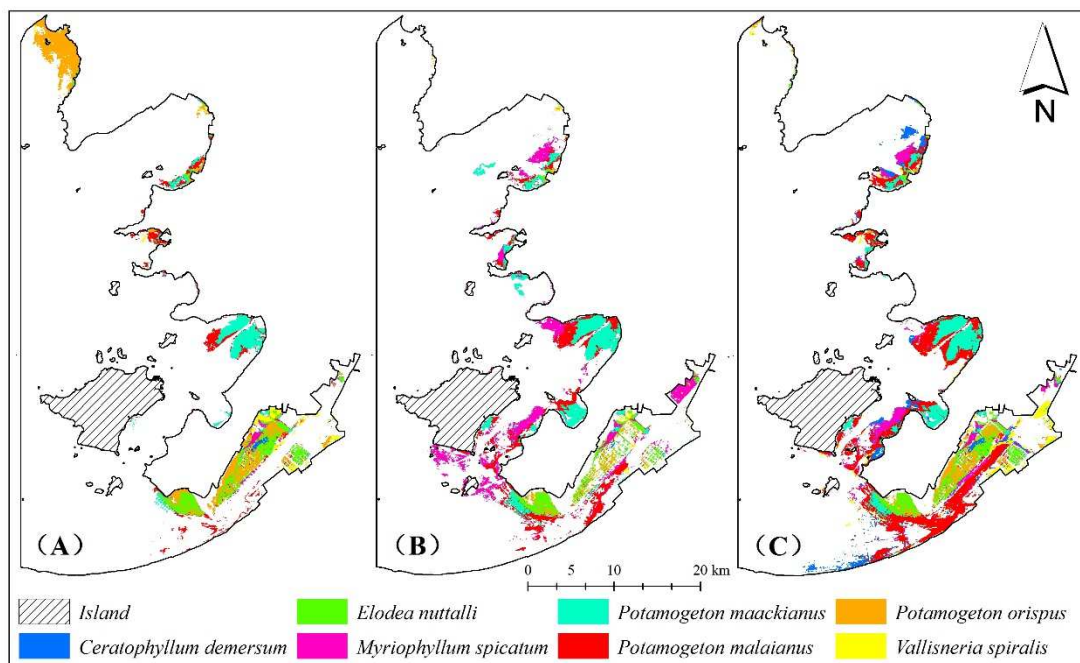
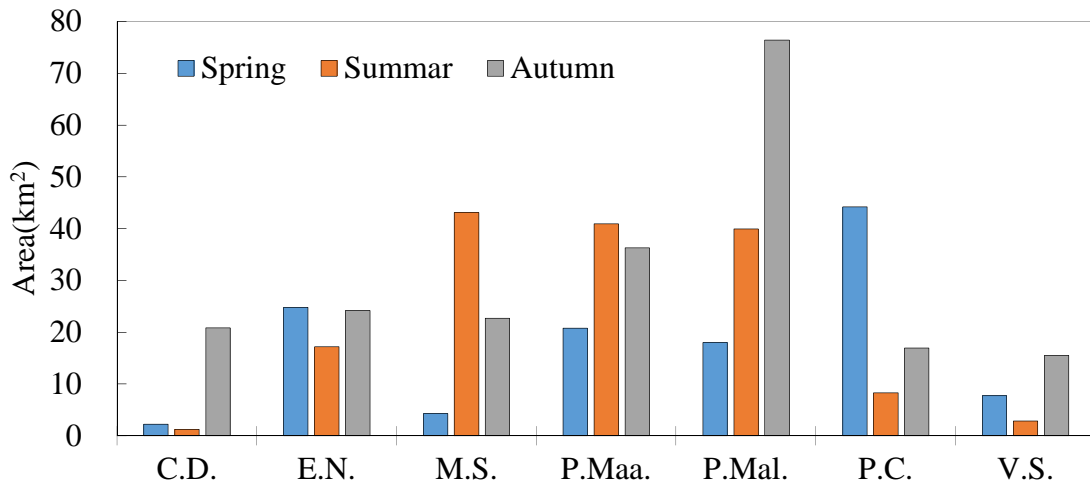


Figure 12. Distribution map of seven SAV species in Spring (A), Summer (B) and



507

508 Figure 13. Distribution area dynamics of seven SAV species with seasons in 2013 in
509 Taihu Lake

510 Note: P.C.=*Potamogeton crispus*; E.N.=*Elodea nuttallii*; M.S.= *Myriophyllum spicatum*;
511 P.Maa.=*Potamogeton maackianus*; C.D. = *Ceratophyllum demersum*; V.S. = *Vallisneria*
512 *spiralis*; P. Mal.= *Potamogeton malaianus*.

513 4. Discussion

514 4.1. Uncertainties, errors and accuracies of classification

515 Mapping studies of aquatic vegetation have been conducted in
516 shallow lake. For example, Ma et al. (2008), Zhao et al (2013) and Luo et
517 al. (2014) proposed different classification methods to map the distribution
518 of emergent, floating-leaved and submerged vegetation in eutrophic Taihu
519 lakes based on moderate resolution images and achieved classification
520 accuracies greater than 80%. However, mapping SAV species is quite
521 challenging because of the limitations of remote sensing and the
522 complexity of the aquatic environment.

523 Fortunately, different SAV species have different phenological
524 characters and life histories. Therefore, based on multi-temporal remote
525 sensing images and the life histories of SAV species, we have proposed a
526 method for mapping and identifying SAV species, but the overall accuracy

was only 68.4% (Table 2) due to many uncertainties. The uncertainties that affect the classification accuracy can be summarized as follows: 1) the limited of the resolution of remote sensing data. On the one hand, spatial resolution can affect classification accuracy because of mixed pixels. Lower spatial resolution can cause more serious mixed pixel phenomena and thus result in larger deviations between the classification and the measured results. On the other hand, the spectral resolution of remote sensing data also directly affects the SAV species mapping accuracy. Figure 14 showed band reflectance of seven SAV species exacted from HJ-CCD image of July 11, 2013. The result showed that it is difficult to classify seven SAV species only using multispectral image. Meanwhile, we also acquired their corresponding situ spectral measurements on July 13, 2013 (Figure 14). It is indicated that there are large differences between the SAV species. Thus, it is possible to classify some species by hyperspectral data. Meanwhile, the studies also suggested that there are tiny spectral differences between SAV species (Han and Rundquist, 2003; Yuan and Zhang, 2006), and only hyperspectral remote sensing data could capture the differences and to then identify SAV species. Therefore, to reduce and eliminate these uncertainties, the resolution of remote sensing data, including spatial resolution and spectral resolutions, must be improved. In future, with the constantly emerging of the hyperspectral sensors, combining our approach, classification accuracies of SAV species would be expected to be further improved. 2) Uncertainty in the aquatic environment. Taihu Lake has experienced significant pollution with high suspension, TN and TP contents, low water transparency, which have caused serious eutrophication and frequent algal blooms. In such a complex aquatic environment, the depth of SAV species from the surface of the water has a significant influence on the classification accuracy. A larger depth can lead to a lower spectral signal-noise ratio and therefore a

lower classification accuracy. For example, *Ceratophyllum demersum* grows at a greater depth from the water surface than other species in even its fast-growing and peak stages, and therefore had the lowest classification accuracy(62.7%). 3) Similar life histories of SAV species. Based on the differences of their life histories, we developed the method for mapping SAV species. Therefore, larger differences of life histories between them can produce higher identification accuracies and vice versa. For example, *Potamogeton crispus* had the highest classification accuracy because it has a distinctly different phenology than the other species. *Myriophyllum spicatum* and *potamogeton maackianus* tended to be misclassified because of their similar life histories. Fortunately, as shown in figure 15, there are significant differences in the red edge and near-infrared region between these species. So it may be a feasible method for reducing the uncertainty and improving their classification accuracies by using hyperspectral data on the basis of our classification results, which would be carried out in our future research.

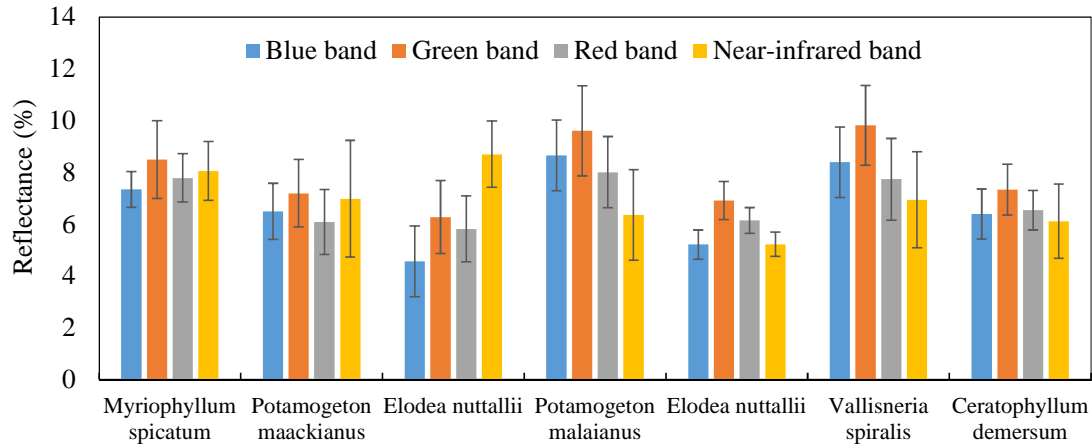


Figure 14. Band reflectance of seven SAV species from HJ-CCD image of July 11, 2013

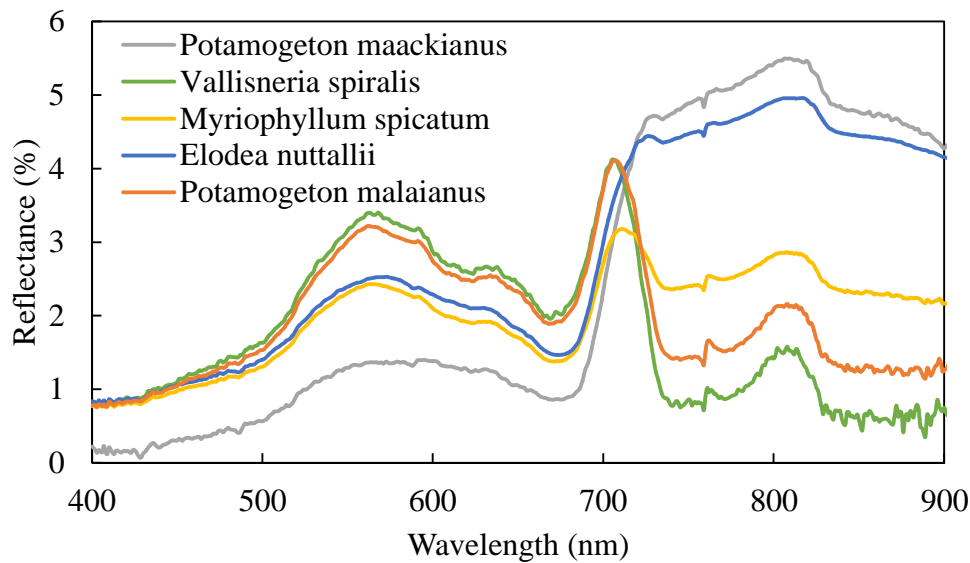


Figure 15. Situ spectral measurements of SAV species on July 13, 2013

4.2. Management and application

Shallow lakes are among the most complex aquatic systems and are known to switch between two stable states: a macrophyte-dominated clear-water state and a phytoplankton-dominated turbid state (Scheffer and van Nes, 2007). Taihu is a typical large, shallow lake, both macrophyte-dominated and phytoplankton-dominated areas exist simultaneously (Liu et al., 2015). However, in recent years, algal blooms have gradually extended its coverage and persisted over longer durations in Taihu Lake. The eutrophication of shallow lakes is characterized by the disappearance of diverse SAV and the dominance of phytoplankton, because SAV and phytoplankton compete for nutrients and light (Dong et al., 2014). Studies have indicated that reasonable distribution of diverse SAV can cause aquatic ecosystems to shift from a turbid algae-dominated state to a clear-water plant-dominated state (Depew et al., 2011; Dong et al., 2014; Hilt et al., 2006). Therefore, the restoration of SAV is an effective method for relieving eutrophication in shallow lakes. Knowing and extracting the physical habitat requirements of the SAV species from their existing habitats is quite crucial for efficient SAV restoration planning. The

interpretation of satellite remote sensing data is the most effective method for mapping the existing habitats of SAV species across an entire lake. In this study, SAV species in Taihu Lake were mapped by combining the characteristics of their life histories and multi-temporal satellite remote sensing data. Although the overall accuracy was only 68.4%, the most suitable ecology and environment conditions and characteristics of the SAV species can be derived from the mapping results. Meanwhile, future work will focus on developing knowledge bases of different SAV species that contains their most suitable ecologies and environment conditions according to their distribution characteristics for guiding SAV restoration work. It is also important determine the historical succession and assess health status and the paludification process of Taihu Lake, based on the the method proposed by this study.

5. Conclusion

Mapping SAV species can capture their most suitable ecology and environment characteristics, which is extremely useful in restoration and management of eutrophic shallow lakes. In this study, the life histories of seven SAV species in Taihu Lake were summarized based on field observations and the literature, and then a multilayer erasing approach for mapping the SAV species mapping was developed based on the life histories of SAV species and multi-temporal satellite remote sensing imagery. Using this approach, the SAV species were mapped in Taihu Lake with an overall accuracy of 68.4% and a kappa coefficient of 0.6306. *Potamogeton crispus* had the highest classification accuracy (PA =75.5% and UA=78.4%), followed by *elodea nuttallii* (PA=70.2% and UA=74.1%), *potamogeton maackianus* (PA =68.9% and UA=68.9%), *potamogeton malaianus* (PA =68.7% and UA=65.2%), *myriophyllum spicatum* (PA =62.7% and UA=60.4%), *potamogeton maackianus* (PA =65.4% and

UA=63%) and *ceratophyllum demersum* (PA =62.7% and UA=69.7%).

Potamogeton malaianus was the most widely distributed species, followed by *Myriophyllum spicatum*, *Potamogeton maackianus*, *Potamogeton crispus*, *Elodea nuttallii*, *Ceratophyllum demersum* and *Vallisneria spiralis*. The distribution area of the seven species changed with the seasons due to their phenological differences. The area covered by SAV was largest in the autumn (212.9 km²), followed by summer (153.5 km²) and spring (122.1km²).

The classification method presented, which is based on multi-temporal satellite images and life histories, is a novel and effective means for identifying SAV species. The classification results should be very helpful for aquatic ecosystem recovery and lake management.

Acknowledgements

This research was supported by the National Natural Science Foundation of China (No. 41301375) and the State Key Program of the National Natural Science Foundation of China (41230853). We thank the Scientific Data Sharing Platform for Lake and Watershed for providing remote sensing data (<http://lake.geodata.cn>) and the Nanjing Institute of Geography and Limnology, Chinese Academy of Sciences.

References

- Angradi, T.R., Pearson, M.S., Bolgrien, D.W., Bellinger, B.J., Starry, M.A., Reschke, C., 2013. Predicting submerged aquatic vegetation cover and occurrence in a Lake Superior estuary. *Journal of Great Lakes Research* 39, 536-546.
- Barko, J.W., Gunnison, D., Carpenter, S.R., 1991. Sediment interactions with submersed macrophyte growth and community dynamics. *Aquatic Botany* 41, 41-65.
- Best, E.P., 1977. Seasonal changes in mineral and organic components of *Ceratophyllum demersum* and *Elodea canadensis*. *Aquatic Botany* 3, 337-348.
- Carr, J., D'Odorico, P., McGlathery, K., Wiberg, P., 2010. Stability and bistability of seagrass ecosystems in shallow coastal lagoons: Role of feedbacks with sediment resuspension and light attenuation. *Journal of Geophysical Research: Biogeosciences* (2005–2012) 115.
- Congalton, R.G., Oderwald, R.G., Mead, R.A., 1983. Assessing Landsat classification accuracy using discrete multivariate analysis statistical techniques. *Photogrammetric Engineering and Remote*

655 Sensing.

656 Depew, D.C., Houben, A.J., Ozersky, T., Hecky, R.E., Guildford, S.J., 2011. Submerged aquatic

657 vegetation in Cook's Bay, Lake Simcoe: Assessment of changes in response to increased water

658 transparency. *Journal of Great Lakes Research* 37, 72-82.

659 Dong, J., Yang, K., Li, S., Li, G., Song, L., 2014. Submerged vegetation removal promotes shift of

660 dominant phytoplankton functional groups in a eutrophic lake. *J Environ Sci (China)* 26, 1699-1707.

661 Duan, H., Loisel, S.A., Zhu, L., Feng, L., Zhang, Y., Ma, R., 2015. Distribution and incidence of algal

662 blooms in Lake Taihu. *Aquatic Sciences* 77, 9-16.

663 Duan, H., Ma, R., Hu, C., 2012. Evaluation of remote sensing algorithms for cyanobacterial pigment

664 retrievals during spring bloom formation in several lakes of East China. *Remote Sens Environ* 126,

665 126-135.

666 Folke, C., Carpenter, S., Walker, B., Scheffer, M., Elmqvist, T., Gunderson, L., Holling, C., 2004. Regime

667 shifts, resilience, and biodiversity in ecosystem management. *Annual Review of Ecology, Evolution,*

668 *and Systematics*, 557-581.

669 Gumbricht, T., 1993. Nutrient removal processes in freshwater submersed macrophyte systems.

670 *Ecological Engineering* 2, 1-30.

671 Han, L., Rundquist, D., 2003. The spectral responses of *Ceratophyllum demersum* at varying depths in

672 an experimental tank. *Int J Remote Sens* 24, 859-864.

673 Hilt, S., Gross, E.M., Hupfer, M., Morscheid, H., Mählmann, J., Melzer, A., Poltz, J., Sandrock, S., Scharf,

674 E.-M., Schneider, S., van de Weyer, K., 2006. Restoration of submerged vegetation in shallow

675 eutrophic lakes – A guideline and state of the art in Germany. *Limnologica - Ecology and*

676 *Management of Inland Waters* 36, 155-171.

677 Hu, L., Hu, W., Deng, J., Li, Q., Gao, F., Zhu, J., Han, T., 2010. Nutrient removal in wetlands with

678 different macrophyte structures in eastern Lake Taihu, China. *Ecological Engineering* 36, 1725-

679 1732.

680 Kunii, H., 1984. Seasonal growth and profile structure development of *Elodea nuttallii* (Planch.) St. John

681 in pond Ojaga-ike, Japan. *Aquatic botany* 18, 239-247.

682 Leite, P.B.C., Feitosa, R.Q., Formaggio, A.R., da Costa, G.A.O.P., Pakzad, K., Sanches, I.D.A., 2011.

683 Hidden Markov Models for crop recognition in remote sensing image sequences. *Pattern*

684 *Recognition Letters* 32, 19-26.

685 Liu, D., Kelly, M., Gong, P., 2006. A spatial-temporal approach to monitoring forest disease spread using

686 multi-temporal high spatial resolution imagery. *Remote Sens Environ* 101, 167-180.

687 Liu, W., Hu, W., Gu, X., 2007. The biomass variation of *Potamogeton malaianus* and its influential factors

688 in Lake Taihu. *Acta Ecologica Sinica* 27, 3324-3333.

689 Liu, X., Zhang, Y., Shi, K., Zhou, Y., Tang, X., Zhu, G., Qin, B., 2015. Mapping Aquatic Vegetation in a

690 Large, Shallow Eutrophic Lake: A Frequency-Based Approach Using Multiple Years of MODIS

691 Data. *Remote Sens-Basel* 7, 10295-10320.

692 Lombardo, P., Cooke, G.D., 2003. *Ceratophyllum demersum*-phosphorus interactions in nutrient

693 enriched aquaria. *Hydrobiologia* 497, 79-90.

694 Luo, J., Li, X., Ma, R., Li, F., Duan, H., Hu, W., Qin, B., Huang, W., 2016. Applying remote sensing

695 techniques to monitoring seasonal and interannual changes of aquatic vegetation in Taihu Lake,

696 China. *Ecol Indic* 60, 503-513.

697 Luo, J.H., Ma, R.H., Duan, H.T., Hu, W.P., Zhu, J.G., Huang, W.J., Lin, C., 2014. A New Method for

698 Modifying Thresholds in the Classification of Tree Models for Mapping Aquatic Vegetation in

699 Taihu Lake with Satellite Images. *Remote Sens-Basel* 6, 7442-7462.

700 Ma, R., Duan, H., Gu, X., Zhang, S., 2008. Detecting aquatic vegetation changes in Taihu Lake, China
701 using multi-temporal satellite imagery. *Sensors* 8, 3988-4005.

702 Module, F., 2009. Atmospheric Correction Module: QUAC and FLAASH User's Guide, Version 4. 7.
703 ITT Visual Information Solutions, Boulder, CO.

704 Murthy, C., Raju, P., Badrinath, K., 2003. Classification of wheat crop with multi-temporal images:
705 performance of maximum likelihood and artificial neural networks. *Int J Remote Sens* 24, 4871-
706 4890.

707 Ni, L., 2001. Growth of *Potamogeton maackianus* under low-light stress in eutrophic water. *Journal of*
708 *Freshwater Ecology* 16, 249-256.

709 Nichols, S.A., Shaw, B.H., 1986. Ecological life histories of the three aquatic nuisance plants,
710 *Myriophyllum spicatum*, *Potamogeton crispus* and *Elodea canadensis*. *Hydrobiologia* 131, 3-21.

711 Olshen, L.B.J.F.R., Stone, C.J., 1984. Classification and regression trees. Wadsworth International Group.

712 Pu, R., Bell, S., Meyer, C., Baggett, L., Zhao, Y., 2012. Mapping and assessing seagrass along the western
713 coast of Florida using Landsat TM and EO-1 ALI/Hyperion imagery. *Estuarine, Coastal and Shelf*
714 *Science* 115, 234-245.

715 Qin, B., 2008. Lake Taihu, China: dynamics and environmental change. Springer Science & Business
716 Media.

717 Rogers, K., Breen, C., 1980. Growth and reproduction of *Potamogeton crispus* in a South African lake.
718 *The Journal of Ecology*, 561-571.

719 Scheffer, M., van Nes, E.H., 2007. Shallow lakes theory revisited: various alternative regimes driven by
720 climate, nutrients, depth and lake size. *Hydrobiologia* 584, 455-466.

721 Shi, K., Zhang, Y., Zhu, G., Liu, X., Zhou, Y., Xu, H., Qin, B., Liu, G., Li, Y., 2015. Long-term remote
722 monitoring of total suspended matter concentration in Lake Taihu using 250m MODIS-Aqua data.
723 *Remote Sens Environ* 164, 43-56.

724 Shuchman, R.A., Sayers, M.J., Brooks, C.N., 2013. Mapping and monitoring the extent of submerged
725 aquatic vegetation in the Laurentian Great Lakes with multi-scale satellite remote sensing. *Journal*
726 *of Great Lakes Research*.

727 Soana, E., Naldi, M., Bartoli, M., 2012. Effects of increasing organic matter loads on pore water features
728 of vegetated (*Vallisneria spiralis* L.) and plant-free sediments. *Ecological Engineering* 47, 141-145.

729 Tadjudin, S., Landgrebe, D.A., 1996. A decision tree classifier design for high-dimensional data with
730 limited training samples, *Geoscience and Remote Sensing Symposium, 1996. IGARSS'96. Remote*
731 *Sensing for a Sustainable Future.*, International. IEEE, pp. 790-792.

732 Wiegleb, G., Kadono, Y., 1989. Growth and development of *Potamogeton malaianus* in SW Japan.
733 *Nordic journal of botany* 9, 167-178.

734 Xiao, C., Wang, X., Xia, J., Liu, G., 2010. The effect of temperature, water level and burial depth on seed
735 germination of *Myriophyllum spicatum* and *Potamogeton malaianus*. *Aquatic Botany* 92, 28-32.

736 Ye, C., Yu, H.-C., Kong, H.-N., Song, X.-F., Zou, G.-Y., Xu, Q.-J., Liu, J., 2009. Community collocation
737 of four submerged macrophytes on two kinds of sediments in Lake Taihu, China. *Ecological*
738 *Engineering* 35, 1656-1663.

739 Yuan, L., Zhang, L., 2006. Identification of the spectral characteristics of submerged plant *Vallisneria*
740 *spiralis*. *Acta Ecologica Sinica* 26, 1005-1010.

741 Zhang, H., Hu, W., Gu, K., Li, Q., Zheng, D., Zhai, S., 2013. An improved ecological model and software
742 for short-term algal bloom forecasting. *Environmental Modelling & Software* 48, 152-162.

743 Zhao, D., Lv, M., Jiang, H., Cai, Y., Xu, D., An, S., 2013. Spatio-Temporal Variability of Aquatic
744 Vegetation in Taihu Lake over the Past 30 Years. PloS one 8, e66365.
745
746